REDISCOVERING STRUCTURAL FOAMS IN INJECTION MOULDING

A. S. Pouzada

Institute for Polymer and Composites
I3N, University of Minho, Guimarães, Portugal

INTRODUCTION

Since the end of World War II injection moulding of thermoplastics gained a leading position in the options to the production of consumer goods and technical articles. This winning combination of technology and modern materials established itself for cases where large production runs and detail precision are specifications. One of the characteristics of the tooling required for this process is its high price that results from the alloy steels and precision machining that are associated to the manufacturing of the moulds; the tooling cost must be paid back by the injection moulded products, this justifying the large production runs that are required for making this technological option economically viable. Nonetheless the industry has been looking for the application of the injection moulding technology to the production of large parts with relatively low cost tooling. A solution that proved itself in the early seventies was the variant of structural foam (Egli 1975) which was implemented in the tank of a domestic washing machine (Anon 1979; Oghoubian and Smart 1990).

Structural foams (SF) are multi-layer materials consisting of two integral skins and a cellular core and can be defined as a rigid cellular plastics structure with load bearing characteristics conferred by the sandwich structure of high specific flexural stiffness/strength ratio (Egli 1972; Moore and Iremonger 1974). Thermoplastic SF may be manufactured by a low pressure short-shot process (typically 65 to 90% of the impression volume), in which an amount of melt containing dissolved gas is injected to produce a short-shot that partially fills the impression (Ahmadi and Hornsby 1984). The gas required for the foaming of the melt is typically generated using a chemical blowing agent (CBA) that releases the gas upon heating. This process is advantageous for producing complex thick and large parts without sink marks, and requiring reduced clamping forces due to the low impression pressures, typically below 4 MPa (compared to 40 MPa in conventional injection moulding) (Eckardt, Alex et al. 1981). Conversely the cycle time is longer and the surface finish is poor (Barzegari and Rodrigue 2009). The injection moulding of SF being a low pressure process is ideal for the production of large area parts. Therefore, it is a viable candidate for light moulding tools, as it is the case of hybrid moulds

(Pouzada 2009).

Recently the Portuguese industry developed an engineering solution for a large plastics part in small series with application in urban furniture, depicted in Fig. 1 (Pouzada, Martinho et al. 2012).

Fig. 1: The root stand for umbrellas

This solution made use of the hybrid mould concept for injection moulds for small production series (Pouzada 2009). In these tools, the moulding blocks are produced by rapid prototyping and tooling (RPT) such as the vacuum casting of epoxy composites. Typically these blocks are produced on epoxy resin with aluminium powder, that have the advantages of easy manufacturing and short delivery time (Bareta, Pouzada et al. 2007). One of the main disadvantages, especially in conventional injection moulding and with relation to conventional steel moulds, is the worst thermal conductivity that leads to longer cycle times.

STRUCTURAL FOAMS AND HYBRID MOULDS

Injection moulded structural foams usually are used in large area mouldings where a radial divergent flow is typical upon filling. Therefore for the study of the processing issues, morphology, and mechanical behaviour bi-dimensional flat mouldings have been used, in some way following the proposal of Stephenson and co-workers in the 70's for studying the performance of this type of mouldings (Stephenson, Turner et al. 1979). In this case, centred gated discs of 155 mm in diameter and 5 mm in thickness (Esteves, Carvalho et al. 2012) and a rectangular moulding with geometrical features (Nogueira, Martinho et al. 2011) were chosen. These moulds were used with a conventional injection moulding machine Engel Victory Spex 50 equipped with a shut-off nozzle to avoid the drooling of the melt.

Hybrid moulds for structural foams

These moulds were signed to work using two mould material combinations for the moulding blocks (core and cavity): conventional all steel mould and hybrid mould. The hybrid mould option was chosen essentially for the following reasons: cheapness of the mould manufacturing cost, and lower thermal conductivity that in this case can be advantageous for the expansion phase of the moulding cycle. The hybrid mould for the circular discs in the injection side has an insulating plate (resin filled with glass fibres) and a

moulding block made in a composite of epoxy Biresin L74 filled with 60wt% aluminium powder as depicted in Fig. 2. The cavity moulding block was produced by vacuum casting and machined to the final geometry of the part.

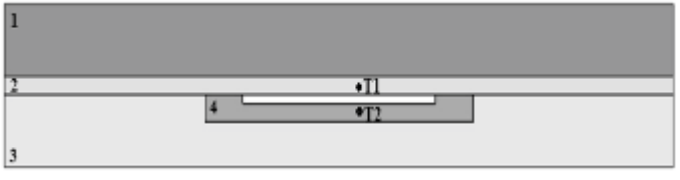

Fig. 2: Hybrid mould configuration and setup of thermocouples: 1-steel injection plate; 2-insulating plate; 3-steel ejection plate; 4-moulding block (resin or steel): T1 and T2 - thermocouples.

The hybrid mould for the more complex rectangular moulding was designed to produce SF mouldings, and to monitor the injection moulding process, namely the expansion force during the filling of the impression (Nogueira, Martinho et al. 2011). The moulding and the structure of the hybrid mould are shown in Fig. 3.

This mould was equipped with a Kistler 9204B load cell (L), three Kistler type N 4008 B 0.4 temperature sensors on the moulding cavity surface, and two thermocouples (T4 and T5) in the inner of moulding insert as shown in Fig. 3. The load cell is used to follow the force associated to the injection of the molten material and its expansion caused by the blowing agent. The temperature sensors are used to measure the mould temperature in the ejection and injection sides, and also to monitor the arrival of the melt at specific position in the mould.

The experience with these moulds was used for the manufacture of the production mould of the industrial component. This mould consists of a core and cavity moulding blocks in an epoxy-aluminium composite (Biresin L74 filled with 60wt% aluminium powder). These moulding blocks are mounted inside of a cylindrical structure (Fig. 4)

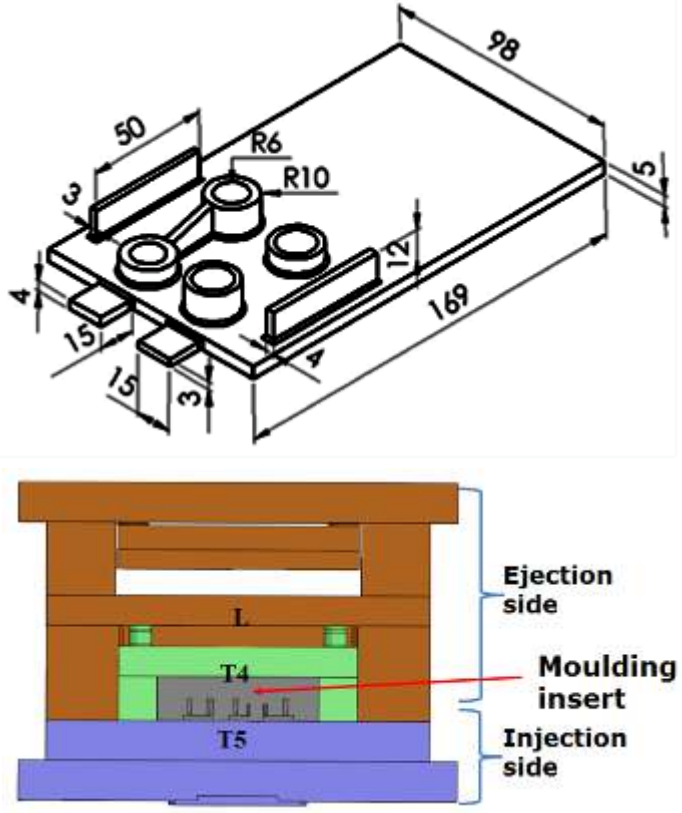

Fig. 3: Structure of the hybrid mould.

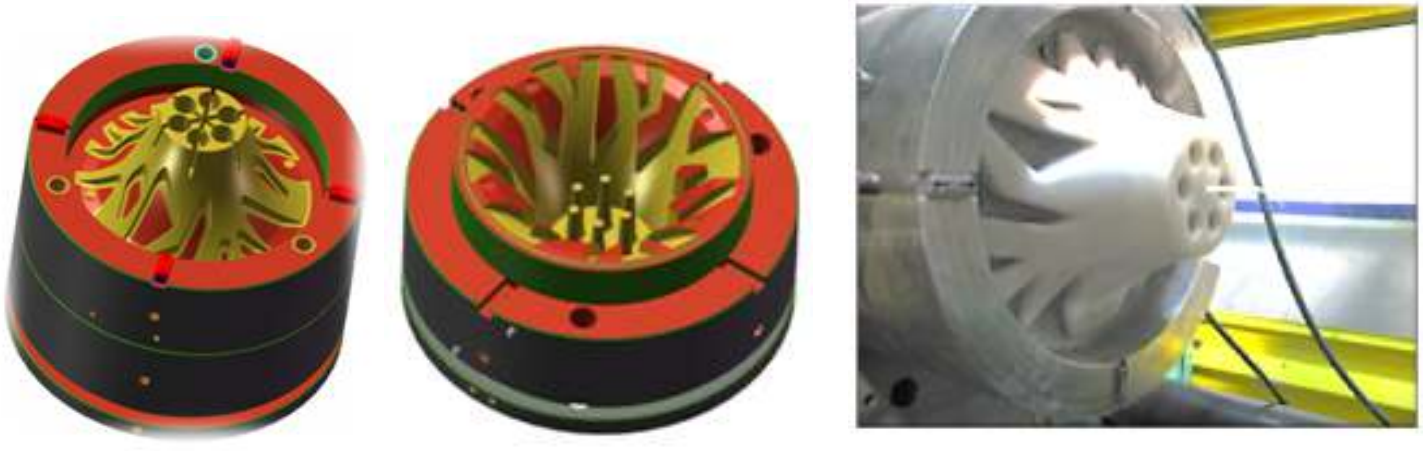

Fig. 4: Prototype mould for production: views of the mould core and cavity, and of an actual moulding prior to ejection from the mould .

Structural foam materials

Most of common thermoplastic materials can be used in the injection moulding of structural foams. The experimental data that are mentioned in this article were obtained from various mouldings (circular discs, rectangular plates with moulding features, and the root stand moulding) that were produced in polypropylene Domolen 1100N (Domo, Belgium) with CBA masterbatch Tracel PP 2200 SP (*PP-SF*), acrilonitrile-butadiene-styrene Kumho 710 (Kumho, Korea) and high impact polystyrene Polystyrol 495F (BASF, Germany) both with CBA masterbatch Tracel IMC 4200SP (Tramaco, Germany), respectively (*ABS-SF*) and (*HIPS-SF*). The CBA has a decomposition temperature in the range of 160-220ºC.

Morphology of structural foams

This study was mostly based on the observation of circular mouldings of PP-SF. The morphology of injection moulding SF develops during the expansion phase of the moulding cycle and consists of two solid skins that form just after the melt contacting the cold mould walls and before the gas cells can expand and a cellular core with cells that often appear distorted by the action of the melt flow. This structure can be observed by light microscopy as in Fig. 5.

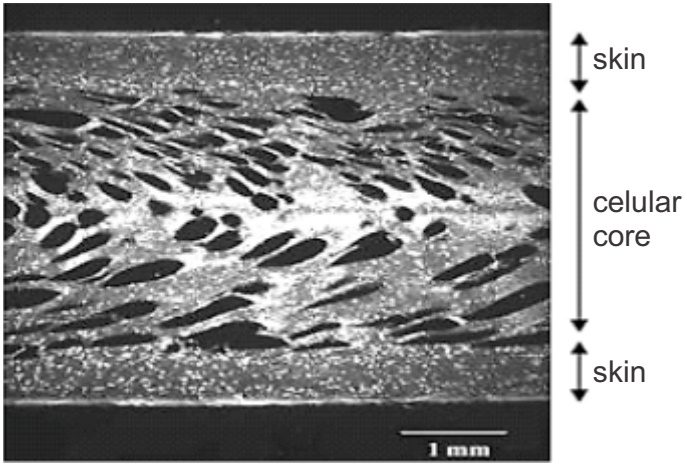

Fig. 5: Morphology of polypropylene SF moulded with a hybrid mould.

Morphological characterization

The typical structure obtained in SF injection moulding is depicted in Fig.5. The structure is characterized by two outer solid layers (skin) and a cellular core. Differently from conventional steel moulds the structure in hybrid mould has cells of larger size with a variety of shapes as it can be seen in Fig. 6.

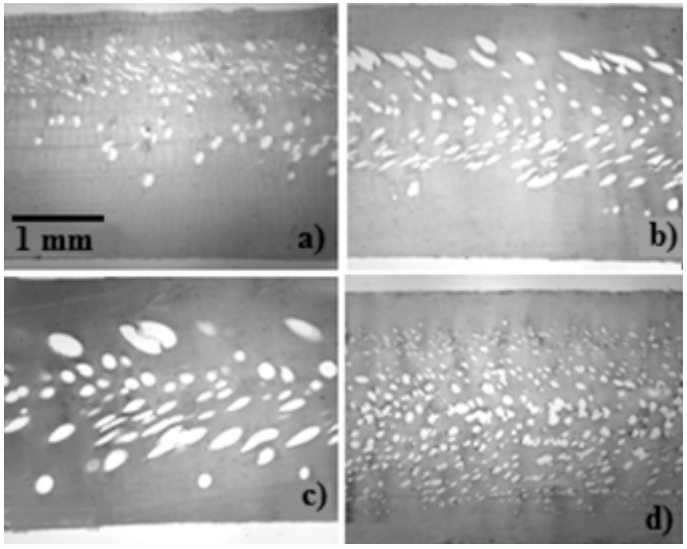

Fig. 6: Polarized light microscopy: influence of the injection temperature on the microstructure of HIPS-SF moulded in hybrid moulds at a) 200ºC; b) 220ºC; and c) 240ºC. The structure in d) was obtained with a conventional steel mould at 220ºC.

The asymmetry in the case of the structures from hybrid moulds is related with the difference of temperature in the two moulding faces. In the core, the cells of hybrid mouldings are approximately 200 μm in diameter and the cells of the steel mouldings are only 80 μm. The cells dimensions are decreasing from the centre to the skin due to the difference in the melt temperature and appear distorted as a result of the fountain flow. With the increase of injection temperature, this phenomenon becomes more pronounced.

Furthermore, the growth of the cell size is evident with increase of the temperature, due to the lower viscosity and the lower resistance to the cell growth as already reported in the literature (Tovar-Cisneros, González-Núñez et al. 2008).

In observations by SEM it was detected the presence of crushed cells and nanopores in the skin region (Fig.7). These can affect the mechanical properties, mainly the impact behaviour, as it will be shown further.

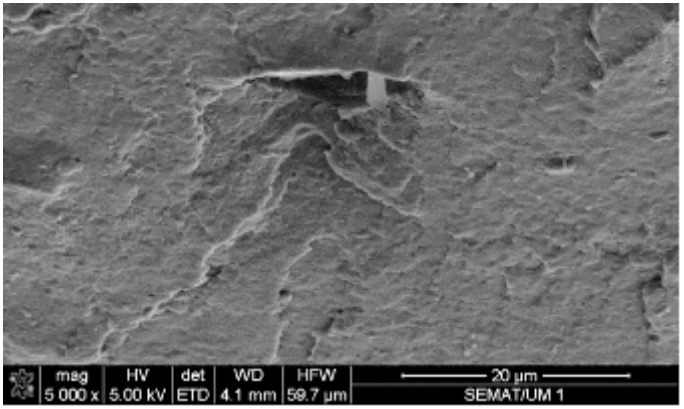

Fig. 7: SEM view of the skin of HIPS-SF moulded at 220ºC with crushed cells and nanopores.

Injection moulding

The study made by Nogueira et al. with the rectangular mouldings using PP-SF showed that SF injection moulding is an unstable process for low levels of mould filling (Nogueira, Martinho et al. 2012). Furthermore at 80% of moulding filling, it was verified that the mouldings were not completely filled.

The use of hybrid moulds, with different materials (composite epoxy and steel) in the core and the cavity, leads to differential shrinkage over the mouldings due to the very different cooling rates in the two mould sides. This results from the thermal conductivity of steel being about 40 $W.m^{-1}.K^{-1}$, whereas in the epoxy composite it is much lower, 0,61 $W.m^{-1}.K^{-1}$.

The successive temperature and pressure cycles, and the ejection friction leads to the degradation in the moulding surface of the epoxy composite moulding block, as shown in Fig. 8.

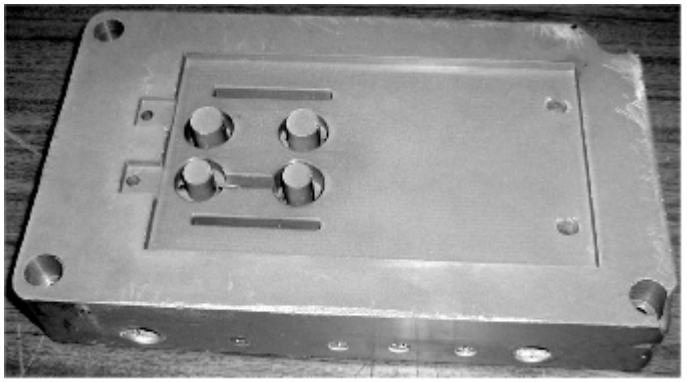

Fig. 8: Composite moulding block after successive injection cycles (Nogueira, Martinho et al. 2012).

This degradation was more noticeable after 1000 injection cycles and especially in the moulding zone with more details.

SF injection moulding monitoring

A typical plot of pressure and clamping force during the injection cycle is shown in Fig. 9.

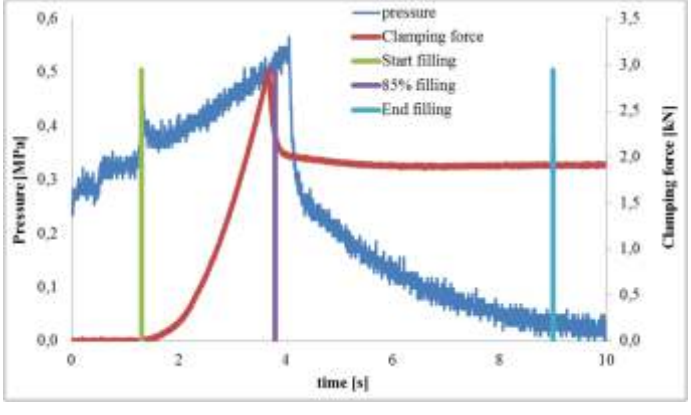

Fig. 9: Pressure and clamping force evolution in PP-SF injection moulding with 85% mould filling (Nogueira, Martinho et al. 2012).

When the injection phase starts the pressure and clamping force increase linearly until the required level of mould filling is reached. The complete filling is promoted by the CBA expansion, with significantly lower pressure and clamping force.

Due to the force in the mould resulting from the injection, there is a peak at the end of the injection phase. It drops abruptly as soon as the injection pressure is released. The clamping force remains constant until the end of the moulding cycle, while the pressure decreases linearly.

Data on the influence of the amount of CBA and percentage of mould filling on the monitored pressure peak and maximum clamping force are shown in Tables 1 and 2.

	3wt% CBA				4wt% CBA			
% fill	80	85	90	95	80	85	90	95
PP	0.52	0.54	0.56	0.58	0.50	0.52	0.54	0.57
ABS	-	0.73	0.79	0.80	-	0.65	0.73	0.73

Table 1: Impression pressure data (Mpa)

	3wt% CBA				4wt% CBA			
% fill	80	85	90	95	80	85	90	95
PP	1.80	2.49	2.91	3.34	2.05	2.30	2.51	3.17
ABS	-	-	3.76	4.99	-	4.06	4.54	5.19

Table 2: Clamping force data (kN)

Upon increasing the level of mould filling, there is a rise in pressure and clamping force in the impression, as a result of the higher volume of material injected. Nevertheless, it is verified that the pressure and clamping force are an order of magnitude smaller than in conventional injection moulding (Nogueira, Martinho et al. 2012).

MECHANICAL PERFORMANCE OF SF MOULDINGS

Many of the applications of injection moulded structural foams is in products where bending strength or impact performance are required, as are the cases of boxes or large mouldings subjected to large loads or impact abuse. These mouldings usually feature large flat surfaces that make appropriate the use of less conventional methods of testing as the plate bending or the falling weight impact.

In these studies the mechanical assessment of amorphous materials, as HIPS-SF and ABS-SF, was made essentially using transversal loading both statically and in impact.

Flexural testing

Having in consideration the limitations that conventional tests in tension and in bending have on the description of the mechanical performance of highly anisotropic mouldings (Stephenson, Turner et al. 1979) non-conventional testing method was used for the plate testing (Pouzada and Stevens 1984). This three-point support flexural test was performed at room temperature using a test rig mounted in an Instron 4505 universal testing machine (Instron, USA), in compression mode (Fig. 10).

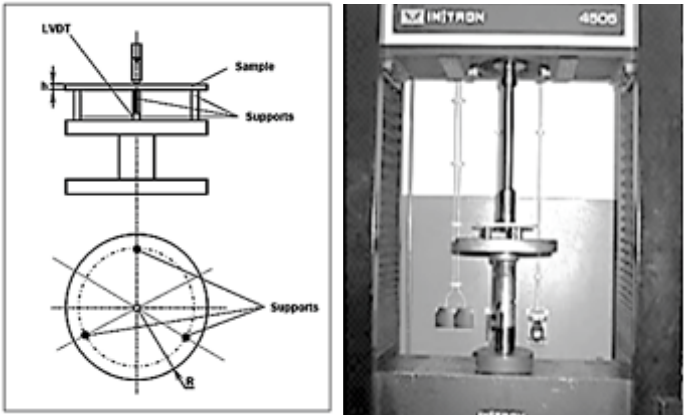

Fig.10: The 3-point support flexural test

The samples were placed on the support base and the load was applied at the centre of sample using a crosshead speed of 5 mm/min. A maximum displacement of 5 mm was imposed, guaranteeing that the sample behaved as a plate in the elastic range. The flexural stiffness data hereafter are the average of five tests.

For isotropic materials that can be mechanically characterized in terms of a modulus (E) and a lateral contraction ratio (v), the flexural stiffness is defined as (Pouzada and Stevens 1984):

$$1)\ C = \frac{E}{(1-v^2)}$$

For small deflections of a circular disc the flexural stiffness, C, can be analytically expressed in terms of the slope of the F/δ trace and the geometrical parameters of the flexural test. In this case it is applicable the Bassali equation:

$$2)\ C = \frac{3R^2\,B(v)}{4\pi h^3}\,S_0$$

where h is the sample thickness, R is the radius of the 3-point support circumference (93.5 mm), B(v) is a function of the Poisson's ratio, which in the range of 0.3 to 0.45 has an average value of 5, for HIPS and ABS that are mechanically similar. The slope, S_0, is the corrected slope of the load versus displacement curve when the support points are not on the periphery of the disc.

In the case of samples overhanging the supports, it is necessary to consider the difference between the radius of the sample and the radius of the support circumference. Given the overhang length ΔR, the support diameter D, and the measured slope, S, the corrected slope, S_0, is calculated as (Pouzada and Stevens 1984):

$$3)\ S_0 = \frac{S}{0.59\left(1-e-\frac{4.1\Delta R}{D}\right)+1}$$

Any mechanical property can be related with morphological characteristics such as density profile and skin ratio (Barzegari and Rodrigue 2009a). Table 3 shows the flexural stiffness, skin ratio and density data of HIPS-SF for various processing conditions. The flexural stiffness, skin ratio and density data present average variations of 5%, 9% and 1%, respectively.

Mould type	Injection temperature	Flexural stiffness [MPa]		Skin ratio [%]	Density [Mg.m^{-3}]	
		SF	100%	SF	SF	100%
Hybrid	200	2277 (119.5)	2614 (164.9)	44.9 (3.7)	0.94 (0.014)	1.028
	200	2237 (88.5)	2568 (14.3)	49.4 (5.6)	0.89 (0.005)	1.029
	240	2132 (135.8)	2542 (51.0)	43.7 (7.5)	0.88 (0.002)	1.027
Steel	220	2081 (190.0)	2327 (93.8)	29.6 (2.6)	0.86 (0.004)	1.028

Table 3: Flexural stiffness, skin ratio and density of HIPS-SF, for various processing conditions.

In general, increasing the injection temperature decreases the skin ratio and the density. The density is related with the amount and distribution of material available to support the applied loads (Lanz et al. 2002) and therefore as it decreases, the flexural stiffness also decreases. The HIPS-SF mouldings in the hybrid mould are slightly stiffer than in the steel mould, due to the higher skin ratio and density.

Impact testing

The impact tests were performed at room temperature with the CEAST 9350 Fractovis Plus instrumented falling-weight equipment (CEAST, Italy) using the following setup: impact weight of 15.765 kg and drop height of 700 mm, leading to an impact speed of

3.7m.s^{-1}. The tests were performed according to the European Standard EN ISO 6603-1.

An example of a fractured HIPS-SF moulding is shown in Fig. 11, the observation suggesting a ductile fracture, as the crack did not propagate in the radial direction.

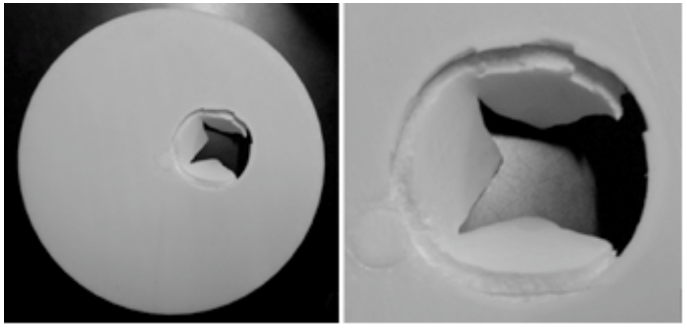

Fig. 11: Fractured HIPS-SF moulding

The effect of the injection temperature on the peak energy observed during impact of mouldings produced at different melt temperature and various mould types is shown in Fig. 12.

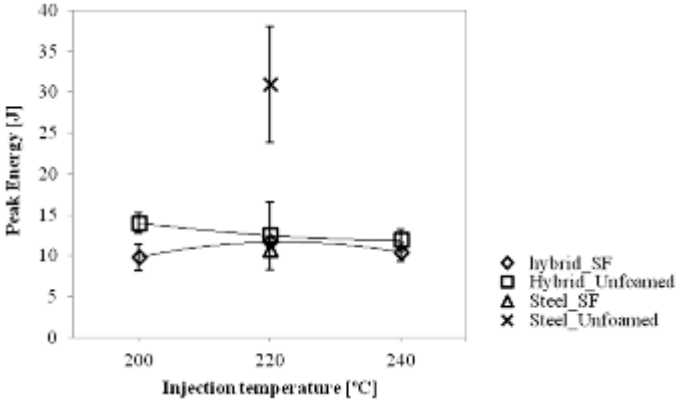

Fig.12: Falling weight impact peak energy of HIPS-SF

As with the flexural properties of HIPS-SF, the falling weight impact resistance is also influenced by the density and the skin thickness. In addition, defects on or near the surface are thought to have major role in determining the peak energy. Raising the injection temperature decreases the peak energy, in accordance to the density reduction.

The occurrence of microcells near to the outer skins may affect the integrity of these outer layers, acting as stress raisers, thus decreasing the impact resistance. The resistance to crack propagation is worst by the formation of large non-uniform cells in the core of the specimens, becoming increasingly evident at high melt temperatures (Ahmadi and Hornsby 1985).

Model prediction

There are analytical models for predicting the mechanical properties once physical and morphological characteristics are known. Barzegari et al. proposed a model to predict the flexural behaviour starting with approximations to the density profile (Barzegari M. P. 2007).To simplify notations, they used normalized parameters, as relative density R, and relative thickness, r:

$$4)\ \frac{\rho c}{\rho s} = R_1;\ \frac{\rho f}{\rho s} = R_2;$$

$$5)\ \frac{\delta_c}{\delta_f} = r;\ \frac{\delta_s}{\delta_f} = 1 - \frac{\delta_s}{\delta_f} = 1 - r$$

where f, s, c are densities and $_f$, $_s$, $_c$ are thicknesses of foam, skin and core, respectively.

Some of those density variation approaches are shown in Fig. 13. These cross-sections represent an approximation of the density profile along the thickness. In this study, the models of Fig. 13c and d are analysed.

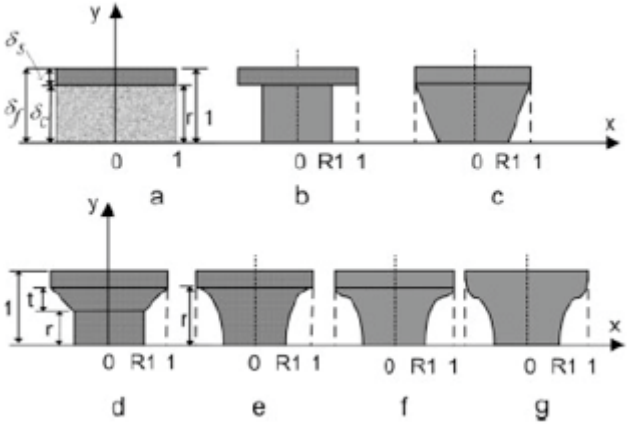

Fig.13: Different approaches of density profiles for SF.

The core density was calculated using the following equations:

$$6)\ \left(\frac{\rho c}{\rho s}\right) = \left(\frac{\rho f}{\rho s} - \frac{\delta_{st}}{\delta_f}\right)\left(1 - \frac{\delta_{st}}{\delta_f}\right)^{-1}$$

$$7)\ _{st} = _{s1} + _{s2}$$

where $_{st}$ is the total skin thickness.

Model C. This model assumes that the core density reaches a minimum at the centre of the beam with a linear variation in the core part. Thus, the normalized flexural modulus is obtained by:

8) $$\frac{E_f}{E_s} = 1 - \frac{r^3}{10}(4 - 3R_1 - R_1)^2$$

Model D. The cross-section of Fig. 13d is decomposed into a three-layer structure. It assumes that the skin density decreases linearly to the core density. An intermediate layer, t, is considered and the core density is uniform. Thus, the normalized flexural modulus is:

9)

$$\frac{E_f}{E_s} = 1 - r^3(1-R_1^2) - r^2 t\,(2 - R_1 - R_1^2) - rt^2\left(\frac{3}{2} - R_1 - \frac{R_1^2}{2}\right) - \frac{t^3}{10}(4 - 3R_1 - R_1^2)$$

Upon using these models, the predicted flexural stiffness of HIPS-SF mouldings was calculated and compared with experimental data as shown in Table 4. The predictions using model D, which assumes a transition layer and a core of uniform density, are not too far from the experimental, with a maximum error of 9%, whereas with model C, that assumes a progressive reduction of density towards the centre of the moulding, the maximum error is about 14%.

Mould type	Injection temperature	Experimental	Predictions			
			$C_{model\ C}$ [MPa]	$C_{model\ D}$ [MPa]	C_C [%]	C_D [%]
Hybrid	H200	2277	2582	2489	11.78	8.51
	H220	2237	2529	2422	11.54	7.64
	H240	2132	2490	2350	14.38	9.27
Steel	S220	2081	2235	1987	6.88	4.51

Table 4: Prediction of flexural stiffness

CONCLUSIONS

Structural foams based on thermoplastic materials are an interesting option for the production of large area mouldings using moulding tools of low cost in comparison to conventional moulds for similar products. The results of recent work exploring the capability of hybrid moulds demonstrated that the combination of these materials with this tool concept is an interesting economical option especially when short series of large products are envisaged.

The mouldings using hybrid moulds can be produced with acceptable reproducibility either in semi-crystalline polymers as polypropylene or amorphous materials as ABS or high impact polystyrene. However the processability is very much dependent on the injection temperature and the percentage of filling prior expansion of the blowing agent that is used. For the materials that were investigated it is suggested that a percentage of filling over 85% is adequate. In these circumstances the maximum required clamping force is only that required to inject the material in the mould prior the expansion of the blowing agent takes place. After that the expansion of the structural foam can be accommodated with a clamping force below 20% of the recorded peak in the injection phase.

The mechanical properties of the structural foam mouldings depend on the morphology of the parts that can be characterised in terms of the 'solid kin / overall thickness' ratio and the average density of the moulding. The impact performance of the structural foam mouldings as measured in the falling weight test

is much lower than solid mouldings in conventional steel moulds and do not depend appreciably on the processing conditions.

The mechanical behaviour can be predicted using analytical models based on morphological properties. These predictions can be made with errors less than 10% using a model that assumes a core with constant density and a transition skin-core layer of varying density.

ACKNOWLEDGEMENTS

The support of the EU program QREN that funded the contract 2010/013307 - project 'Hybridmould 21' is acknowledged.

The contribution of the Institute for Polymers and Composites of the University of Minho was supported by the Strategic Project PEst-C/CTM/LA0025/2013.

REFERENCES

[1] Ahmadi, A. A. and P. R. Hornsby (1984). "Moulding and Characterization studies with polypropylene structural foam. I. Structure-property interrelationships." Plast. Rubber Process. Appl. 5(1): 35-49.

[2] Ahmadi, A. A. and P. R. Hornsby (1985). "Moulding and characterization studies with polypropylene structural foam. II. The Influence of Processing Conditions on Structure and Properties." Plast. Rubber Process. Appl. 5(1): 51-59.

[3] Anon. (1979). Coupled glass-reinforced structural foam 'Propathene' - a new engineering material. Propathene Scene. I. P. Division. Welwyn Garden City, Imperial Chenical Insdustries Limited. 34.

[4] Bareta, D. R., A. S. Pouzada, et al. (2007). The effect of rapid tooling materials on mechanical properties of tubular mouldings. PMI 2007 - Int. Conf. on Polymers & Moulds Innovations. Gent/Belgium.

[5] Barzegari M. P., D. R. (2007). "The effect of density profile on the flexural properties of structural foams." Polymer Engineering & Science.

[6] Barzegari, M. R. and D. Rodrigue (2009). "The Effect of Injection Molding Conditions on the Morphology of Polymer Structural Foams." Polymer Engineering and Science 49, 5: 949-959.

[7] Barzegari, M. R. and D. Rodrigue (2009). "Flexural behavior of asymmetric structural foams." Journal of Applied Polymer Science 113: 3103-3112.

[8] Eckardt, H., K. Alex, et al. (1981). "Structural and coinjection foam molding." Advances in Polymer Technology 1(2): 40-49.

[9] Egli, E. A. (1972). "Design Properties of Structural Foam." Journal of Cellular Plastics 8(5): 245-249.

[10] Esteves, F. R., T. A. Carvalho, et al. (2012). The influence of processing conditions on the aesthetical, morphological and mechanical properties of SF mouldings of high-impact polystyrene (HIPS-SF). PMI 2012 - Int. Conf. on Polymers & Moulds Innovations. L. Cardon. Gent, Belgium: 54-60.

[11] Esteves, F. R., A. S. Pouzada, et al. (2013). "Characterization of Polypropylene Structural Foams for Large Part Applications." Materials Science Forum 730-732: 981-987.

[12] Lanz, R. W., S. N. Melkote, et al. (2002). "Machinability

of rapid tooling composite board." Journal of Materials Processing Technology 127(2): 242-245.

[13] Moore, D. R. and M. J. Iremonger (1974). "The Prediction of the Flexural Rigidity of Sandwich Foam Mouldings." Journal of Cellular Plastics 10(5): 230-236.

[14] Nogueira, A. A., P. G. Martinho, et al. (2011). A study on the mouldability of technical parts using hybrid moulds and structural foams. Innovative Developments in Virtual and Physical Prototyping. P. J. e. a. Bartolo. London, CRC Press/Balkema: 399-404.

[15] Nogueira, A. A., P. G. Martinho, et al. (2012). Studies on the mouldability of structural foams in hybrid moulds. PMI 2012 - Int. Conf. on Polymers & Moulds Innovations. L. Cardon. Ghent, Belgium: 116-121.

[16] Oghoubian, R. and J. Smart (1990). "Out-of-plane bending of faceted cylinder end plates." The Journal of Strain Analysis for Engineering Design 25(2): 95-101.

[17] Pouzada, A. S. (2009). "Hybrid moulds: a case of integration of alternative materials and rapid prototyping for tooling." Virtual and Physical Prototyping 4(4): 195 - 202

[18] Pouzada, A. S., P. G. Martinho, et al. (2012). "Hybridmould 21 – from a mould concept to reality." O Molde 93: 29-37.

[19] Pouzada, A. S. and M. J. Stevens (1984). "Methods of generating flexural design data for injection moulded plates." Plastics and Rubber Processing and Applications 4(2): 181-187.

[20] Stephenson, R. C., S. Turner, et al. (1979). "The load capability of short fiber thermo-plastics composites - a new practical system of evolution " Polymer Engineering & Science 19: 173.

[21] Tovar-Cisneros, C., R. González-Núñez, et al. (2008). "Effect of mold temperature on morphology and mechanical properties of injection molded HDPE structural foams." Journal of Cellular Plastics 44(3): 223-237.